



## The ionic strength effect on the DNA complexation by DOPC – gemini surfactants liposomes

Petra Pullmannová<sup>a,b,\*</sup>, Margarida Bastos<sup>c</sup>, Guangyue Bai<sup>c</sup>, Sergio S. Funari<sup>d</sup>, Ivan Lacko<sup>e</sup>, Ferdinand Devínsky<sup>e</sup>, José Teixeira<sup>f</sup>, Daniela Uhríková<sup>b</sup>

<sup>a</sup> Department of Physical Chemistry, Faculty of Chemical and Food Technology, Slovak University of Technology, Radlinského 9, SK-812 37 Bratislava, Slovakia

<sup>b</sup> Department of Physical Chemistry of Drugs, Faculty of Pharmacy, Comenius University, Odbojárov 10, SK-832 32 Bratislava, Slovakia

<sup>c</sup> CIQ(UP), Department of Chemistry and Biochemistry, Faculty of Sciences, University of Porto, Rua do Campo Alegre 687, P-4169-007, Porto, Portugal

<sup>d</sup> HASYLAB at DESY, Notkestr. 85, D-22607 Hamburg, Germany

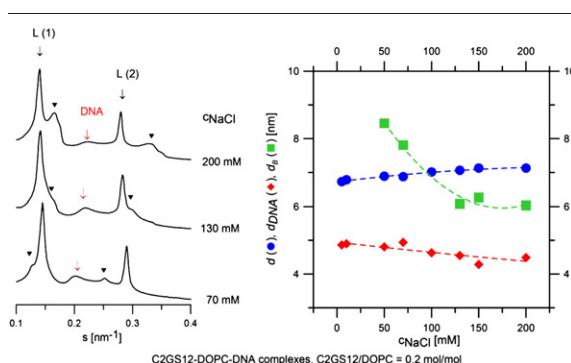
<sup>e</sup> Department of Chemical Theory of Drugs, Faculty of Pharmacy, Comenius University, Odbojárov 10, SK-832 32 Bratislava, Slovakia

<sup>f</sup> Laboratoire Léon Brillouin (CEA-CNRS), CEA Saclay, F-91191 Gif-sur-Yvette Cedex, France

### HIGHLIGHTS

- Gemini surfactant – DOPC liposomes condense DNA at physiologically relevant ionic strength.
- In addition to the condensed lamellar  $L_C^c$  phase, a coexisting lamellar phase  $L_B$  was also identified in formed complexes.
- Sufficiently high surface charge density and method of complex preparation are key parameters to avoid the phase coexistence.

### GRAPHICAL ABSTRACT



### ARTICLE INFO

#### Article history:

Received 13 July 2011

Received in revised form 1 September 2011

Accepted 4 September 2011

Available online 22 September 2011

#### Keywords:

DOPC

DNA

Gemini surfactant

Ionic strength

Small angle X-ray diffraction

Isothermal titration calorimetry

### ABSTRACT

Liposome dispersions obtained from the mixture of gemini surfactants of the type alkane- $\alpha,\omega$ -diyl-bis(alkyldimethylammonium bromide) and helper lipid DOPC create complexes with DNA showing a regular inner microstructure, identified by small angle X-ray diffraction as condensed lamellar phase ( $L_C^c$ ). In addition to the  $L_C^c$  phase, a coexisting lamellar phase  $L_B$  was also identified in the complexes formed, with periodicities in the range  $\sim 8.8$ – $5.7$  nm, at ionic strengths corresponding to 50–200 mM NaCl. The periodicities of  $L_B$  phase did not correspond to those identified in liposome dispersion without DNA using small angle neutron scattering. The observed phase separation is shown to depend on the interplay between the surface charge density of cationic liposomes, ionic strength and method of complex preparation. The effect of ionic strength on complex formation was studied by isothermal titration calorimetry and zeta potential measurements. High ionic strength reduces the fraction of bound DNA in the complexes, and the isoelectric point is attained at a ratio of DNA/gemini surfactant which is lower than the one that can be estimated by calculation based on nominal charges of CLs and DNA.

© 2011 Elsevier B.V. All rights reserved.

**Abbreviations:** CLs, cationic liposomes; CnGSm, gemini surfactant alkane- $\alpha,\omega$ -diyl-bis(alkyldimethylammonium bromide); DOPC, dioleoylphosphatidylcholine; DPPC, dipalmitoylphosphatidylcholine; CTDNA, calf thymus DNA; HTDNA, DNA from herring testes;  $L_C^c$ , condensed lamellar phase;  $L_B$ , additional lipid phase with lamellar structure; SAXD, small angle X-ray diffraction; WAXD, wide angle X-ray diffraction; SANS, small angle neutron scattering; ITC, isothermal titration calorimetry.

\* Corresponding author at: Department of Physical Chemistry of Drugs, Faculty of Pharmacy, Comenius University, Odbojárov 10, SK-832 32 Bratislava, Slovakia. Tel.: +421 250117289.

E-mail address: [pullmannova@fpharm.uniba.sk](mailto:pullmannova@fpharm.uniba.sk) (P. Pullmannová).

## 1. Introduction

Cationic liposomes (CLs) condense nucleic acids into complexes with a regular inner microstructure, capable of passing through somatic cell's membrane. As gene delivery carriers, they were used for the first time by Felgner et al. [1]. Since the first study, many cationic lipids have been synthesized, as potential candidates for gene delivery vectors. Physico-chemical properties, structure, transfection efficiency and relations between them have been intensively investigated. To design complexes with the desired microstructure and enhanced transfection efficiency, the interplay of the electrostatic, elastic, and entropic-mixing forces has to be considered [2–6]. The helper neutral lipid used together with cationic components moderates the colloidal and structural properties of the complex and facilitates the transport through the cell's membrane [7,8]. Fluidity, hexagonal-phase-forming propensity and fusogenic potential of the helper lipid play the major role in the enhanced transfection efficiency [4,9]. DNA – cationic liposome complexes create three types of organized microstructures: i) condensed lamellar phase ( $L_\alpha^C$ ) with ordered DNA monolayers intercalated between lipid bilayers [10,11]; ii) condensed columnar inverted hexagonal phase ( $H_{II}^C$ ) with linear DNA molecules surrounded by lipid monolayers forming inverted cylindrical micelles arranged on a hexagonal lattice [12]; iii) condensed columnar hexagonal phase ( $H_I^C$ ) with cylindrical micelles arranged in an hexagonal lattice, and DNA strands filling the interspace between micelles, forming a honeycomb structure [13].

Kirby et al. [14] introduced gemini surfactants as possible gene delivery carriers. These amphiphilic compounds attract the scientific interest because they represent a useful group of surfactants for applications where precisely designed aggregation properties are required [15]. The complexes based on gemini surfactants alkane- $\alpha,\omega$ -diyl-bis(alkyldimethylammonium bromide) (CnGS $m$ , Fig. 1) have shown good transfection activity *in vitro* [16] and *in vivo* [17]. CnGS $m$ , with two alkyl chains (where  $m$  is the number of carbons in the alkyl chain) and two quaternary ammonium groups, connected by a polymethylene chain referred to as a spacer ( $n$  is the number of carbons in the spacer) were used to build a simple model system for our study.

We have used small and wide angle X-ray diffraction (SAXD and WAXD) to characterize the microstructure of complexes prepared from the CnGS12 surfactant and DNA, using dioleoylphosphatidylcholine (DOPC) as a helper lipid, mixed at a ratio corresponding to the calculated isoelectric point. In this study we focused on the structural diversity induced by the liposome composition or bulk solution's conditions. The dependence of the process of DNA condensation on the DNA/C2GS12 molar ratio and bulk solution's conditions was monitored by isothermal titration microcalorimetry (ITC) and zeta potential measurements. Small angle neutron scattering (SANS) was used to characterize the C2GS12–DOPC dispersion.

Aiming to adopt physiologically relevant conditions in the study we decided to work initially at the ionic strength corresponding to a NaCl concentration of 150 mM. However, the preliminary experiments have alerted the need of a more detailed investigation of the high salt concentration's effects. Until now the studies of the effect of ionic strength on DNA – cationic liposomes complexes (DNA–CLs)

have shown that the increase in ionic strength reduces the amount of DNA which the CLs are able to bind [3,18,19]. At sufficiently high salt concentration the charge screening precludes the interaction of DNA with CLs. Other study reported that both under optimum medium conditions for routine transfection as well as in water, the formed DNA–CLs complexes carry negative charges [20]. It has also been reported that the zeta potential of the complexes formed in water can be significantly lowered by the addition of NaCl [21].

DNA was found to induce microscopic lateral phase segregation in mixed lipid membranes [22–24]. The segregation is seen as the formation of lipid microdomains having different composition. In the presence of electrostatic interactions between the lipid membrane and the polymer, the segregation could be induced by the attraction between the oppositely charged components leading to spatial changes in the distribution of the charged compounds in the membrane [25].

## 2. Materials and methods

### 2.1. Chemicals

Neutral phospholipid DOPC (1,2-dioleoyl-*sn*-glycero-3-phosphocholine,  $M_r = 786.15$ ) was purchased from Avanti Polar Lipids, Inc., USA, highly polymerized calf thymus DNA (sodium salt) type I (CTDNA, average  $M_r$  of nucleotide = 308) and DNA (sodium salt) type XIV from Herring testes (HTDNA, average  $M_r$  of nucleotide = 308) from Sigma Chemicals Co., USA. Alkane- $\alpha,\omega$ -diyl-bis(dodecyldimethylammonium bromide) surfactants (CnCS12,  $n = 2, 3, 4$ ) were prepared as described in [26] and purified by manifold crystallization from a mixture of acetone and methanol. The NaCl and NaOH of analytical purity were obtained from Lachema, Brno, Czech Republic.  $^2\text{H}_2\text{O}$  (99.9%) was purchased from Merck, Germany. The chemicals were of the analytical grade and were used without further purifications. The aqueous solutions were prepared with redistilled water, pH ~6 except the solutions for isothermal titration microcalorimetry, which were prepared using Millipore water.

### 2.2. Preparation of cationic liposomes

DOPC and CnGS12 were dissolved in organic solvent (mixture of chloroform and methanol at volume ratio = 3:1). The appropriate amounts of organic stock solutions were mixed to obtain the desired ratio (CnGS12/DOPC = 0.15–0.5 mol/mol). The solvent was evaporated under a stream of gaseous nitrogen and its residue removed by a vacuum. The dry mixture was hydrated by the NaCl solution of appropriate concentration for 12 h. Afterwards the mixture was homogenized (by vortexing, freezing–thawing cycles or sonication in an ultrasound bath) until an opalescent dispersion was created. We tested the size and polydispersity of prepared cationic liposomes (CLs) by the dynamic light scattering measurements using the Nano ZetaSizer 5000. We obtained the values of diameter ~250 nm for the CLs at ratio C2GS12/DOPC = 0.3 in 5 mM NaCl and ~1000 nm in 70 mM NaCl. Both dispersions have shown low polydispersity in diameter. The control samples of pure DOPC were prepared in the same manner and we obtained a milky dispersion of multilamellar liposomes. Liposome dispersions for SANS experiments were prepared at phospholipid concentration 10 mg/ml in the same manner except the usage of  $^2\text{H}_2\text{O}$  instead of  $\text{H}_2\text{O}$ .

### 2.3. Preparation of DNA solutions

The stock solutions were prepared by dissolving CTDNA or HTDNA at concentration 2 mg/ml or 3 mg/ml, respectively, both in 5 mM NaCl or 200 mM NaCl solution. To obtain the intermediate values of NaCl concentration of DNA solution, we mixed the stock solutions of DNA in 5 mM NaCl and 200 mM NaCl at appropriate ratios. The

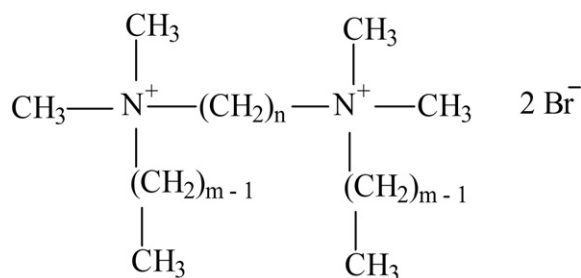


Fig. 1. The structure of alkane- $\alpha,\omega$ -diyl-bis(alkyldimethylammonium bromide) (CnGS $m$ ).

precise value of DNA concentration was determined spectrophotometrically (Hewlett Packard 8452A Diode array spectrophotometer), according to equation:  $c_{\text{DNA}} = A_{260} \times 4.7 \times 10^{-5}$  [g/ml], where  $A_{260}$  is the absorbance at wavelength  $\lambda = 260$  nm. The concentration of DNA is referred as molar concentration of DNA base pairs (mol bp). The purity of DNA was checked by measuring the absorbance  $A_{\lambda}$  at  $\lambda = 260$ , 230 and 280 nm. We have obtained for CTDNA the values of  $A_{260}/A_{230} = 2.23$  and  $A_{260}/A_{280} = 1.76$  and for HTDNA  $A_{260}/A_{230} = 2.26$  and  $A_{260}/A_{280} = 1.82$ .

#### 2.4. Small- (SAXD) and wide-angle (WAXD) synchrotron radiation diffraction measurements

The samples for SAXD and WAXD measurements except control samples were prepared as following. The CTDNA solution was added to the liposome dispersion DNA in two manners, either by drop-by-drop addition of DNA solution, or by addition of all the appropriate amount of DNA solution at once. After each addition of DNA solution the sample was shortly mixed and a precipitate was created spontaneously during the mixing. The samples were prepared at the calculated isoelectric point DNA/CnGS12 = 1 mol bp/mol and stored in a refrigerator at 2–6 °C or in a freezer at approximately –20 °C. Before measurement, the sample was shortly centrifuged, the sediment was placed between two Kapton foil (Dupont, France) windows of a sample holder for X-ray diffraction. A few drops of bulk solution were added to the sample and the holder was enclosed. Small- (SAXD) and wide-angle (WAXD) synchrotron radiation diffraction experiments were performed at the soft condensed matter beamline A2 at HASYLAB at the Deutsches Elektronen Synchrotron (DESY) in Hamburg (Germany), using a monochromatic radiation of wavelength  $\lambda = 0.15$  nm. The evacuated double-focusing camera was equipped with a linear position sensitive detector for WAXD and a 2D MarCCD detector for SAXD. The sample was equilibrated at selected temperature (20 °C) for 5 min before exposure to radiation. The raw data were normalized against the incident beam intensity using the signal intensity measured in an ionization chamber. The SAXD detector was calibrated using Ag behenate [27] and the WAXD detector by tripalmitin [28,29]. Each diffraction peak of SAXD region was fitted with a Lorentzian above a linear background. The WAXD pattern of all measured samples exhibited one wide diffuse scattering in the ranges  $\sim 1.8$ – $3.2$  nm<sup>–1</sup>, characteristic for liquid-like carbon chains of phospholipid and CnGS12 molecules. We do not show WAXD patterns. Typical SAXD patterns of condensed lamellar phase of DNA-CLs complexes exhibit a set of sharp periodically spaced reflections at  $s_l = l/d$  ( $l = 1, 2, 3, \dots$ ) and a broad peak at  $s_{\text{DNA}} = 1/d_{\text{DNA}}$ . The repeat distance  $d$  corresponding to the distance of lipid bilayers was determined according to equation  $d = 1/s_1$ , where  $s_1$  is the first order reflection's maximum. The DNA–DNA distance of periodically spaced DNA strands was determined according to the equation  $d_{\text{DNA}} = 1/s_{\text{DNA}}$ . The repeat distance  $d = d_L + d_W$  involves the thickness of phospholipids bilayer  $d_L$  and the thickness of hydrated layer of DNA strands  $d_W$ .

#### 2.5. Isothermal titration calorimetry

Isothermal titration microcalorimetry (ITC) was used to characterize the thermodynamics of the interaction of DNA with cationic liposomes. The water bath and peripheral units were built at Lund University, and a twin heat conduction calorimeter (ThermoMetric AB, Järfälla, Sweden) was used with a 1 mL titration cell equipped with a plastic stirrer (turbine type). The detailed calorimetric set-up and basic procedure has been described previously [30]. The calibration and the time constant were determined through electrical calibration experiments, using an insertion heater [31]. The detailed calorimetric procedure and curve correction have been described elsewhere [30,32]. HTDNA solution contained in a Hamilton syringe with a computer-operated syringe drive is added step-wise to a

liposome dispersion ( $V = 0.899 \pm 0.003$  ml) contained in the titration cell. Liposome dispersions were prepared as referred above; the concentration of C2GS12 in the sample was calculated from its mass, weighted in the analytical balance. Each titration run consisted of 25 successive injections ( $V_{\text{inj}} = 12.511 \pm 0.002$   $\mu$ l) of a 3 mg/ml HTDNA stock solution, at 7-min intervals (injections with 20-min interval did not reveal the presence of slow reactions). Experiments performed in the fast titration mode with 7-min intervals required the deconvolution of the resulting curves prior to integration [30]. Resulting thermograms were evaluated using the Origin software, and the obtained peak areas used to calculate the calorimetric enthalpies  $\Delta H_{\text{obs cond}}$  (kJ/mol DNA base pairs) through the previously obtained calibration constant. The obtained enthalpies  $\Delta H_{\text{obs cond}}$  were corrected for the dilution effects,  $\Delta H_{\text{obs dil}}$ , (also expressed in kJ/mol DNA base pairs) which were taken to be the average of the peaks of reverse sign, observed after the “beyond-the-endpoint” of the calorimetric profile [6]. Thus, the reported enthalpy change is  $\Delta H = \Delta H_{\text{obs cond}} - \Delta H_{\text{obs dil}}$  (kJ/mol DNA base pairs).

#### 2.6. Zeta potential measurement

The zeta-potential of HTDNA-CLs complexes was measured by electrophoretic mobility of particles using a Nano ZetaSizer 5000 (Malvern Instruments, UK). The measurements were performed in a polycarbonate DTS 1060 C cell (750  $\mu$ l), at a temperature of 25 °C, and at a scattering angle of 90°. The solvent viscosity and refractive index values were 0.89 cP and 1.331, respectively. The zeta potential was evaluated by Malvern software using the Smoluchowski model. The HTDNA stock solutions and liposome dispersion were diluted 80 times with NaCl solution of corresponding concentration. Liposome dispersion of 0.7 ml and HTDNA in various proportions were mixed in eppendorfs and transferred into the polycarbonate DTS 1060C cell, and the zeta-potential measured afterwards.

#### 2.7. Small angle neutron scattering

The SANS experiments were performed on the PAXE spectrometer at LLB (CEA Saclay, France). The samples of CLs at C2GS12/DOPC = 0.2 mol/mol were filled into 2 mm thick quartz cells (Hellma, Germany) for SANS. The sample to detector distance was 1.3 and 5.05 m, respectively, and the neutron wavelength was  $\lambda = 0.6$  nm ( $\Delta\lambda/\lambda = 10\%$ ) covering the scattering vector range  $0.05$ – $3$  nm<sup>–1</sup>. The acquisition time for one sample was 30 min. The normalized SANS intensity  $I(q)$  as a function of the scattering vector modulus  $q$  was obtained as described previously [33]. The scattering curves were further treated according to [34], for more details see supplementary material.

### 3. Results

#### 3.1. SAXD measurements

Samples for SAXD experiments were prepared at the calculated isoelectric point based on nominal charges of each species, corresponding to the molar ratio DNA/CnGS12 = 1 mol bp/mol. We used fully hydrated DOPC as a control sample for the experiments. Cylinder-shaped molecules of DOPC form a lamellar phase  $L_{\alpha}$  with the repeat distance  $d = 6.35 \pm 0.1$  nm at 20 °C (not shown).

##### 3.1.1. C3GS12-DOPC-CTDNA complexes at various molar ratios C3GS12/DOPC

We prepared a series of samples using CTDNA and CLs composed of C3GS12-DOPC at varying molar ratios of C3GS12/DOPC from 0.1 to 0.5 mol/mol. DNA solution was added stepwise to the liposome dispersion as described above. The structure of complexes C3GS12-DOPC-CTDNA was studied under conditions of physiologically relevant ionic strength of 150 mM NaCl bulk solution. Gemini surfactant

with the spacer of 3 carbons was chosen because of the highest transfection efficiency expressed within the homological series with different spacer's length *in vitro* [35] and good transfection activity *in vivo* [17]. The SAXD patterns of complexes C3GS12-DOPC-CTDNA at 20 °C are shown in Fig. 2. Two sharp periodically spaced reflections L(1) and L(2) present in all diffraction patterns refer to the lamellar arrangement of lipid bilayers, the broad peak in between them marked by a red arrow arises from the regular ordering of DNA strands. All the samples form  $L_\alpha^c$  phase, typical for complexes based on DOPC [3]. At the molar ratio C3GS12/DOPC  $\leq 0.36$  we observed an evidence of peak splitting and coexistence of  $L_\alpha^c$  phase with another  $L_B$  phase or with two distinguishable  $L_B$  phases having regular lamellar arrangement and slightly different  $d_B$ . Weak ordering and no detectable reflection for DNA–DNA correlation are characteristic of  $L_B$  phases. The structural parameters  $d$ ,  $d_B$ , and  $d_{DNA}$  of  $L_\alpha^c$  and additional  $L_B$  phases were evaluated and are shown in Fig. 3. The repeat distance  $d$  as a function of the molar ratio C3GS12/DOPC decreases from 7.28 to

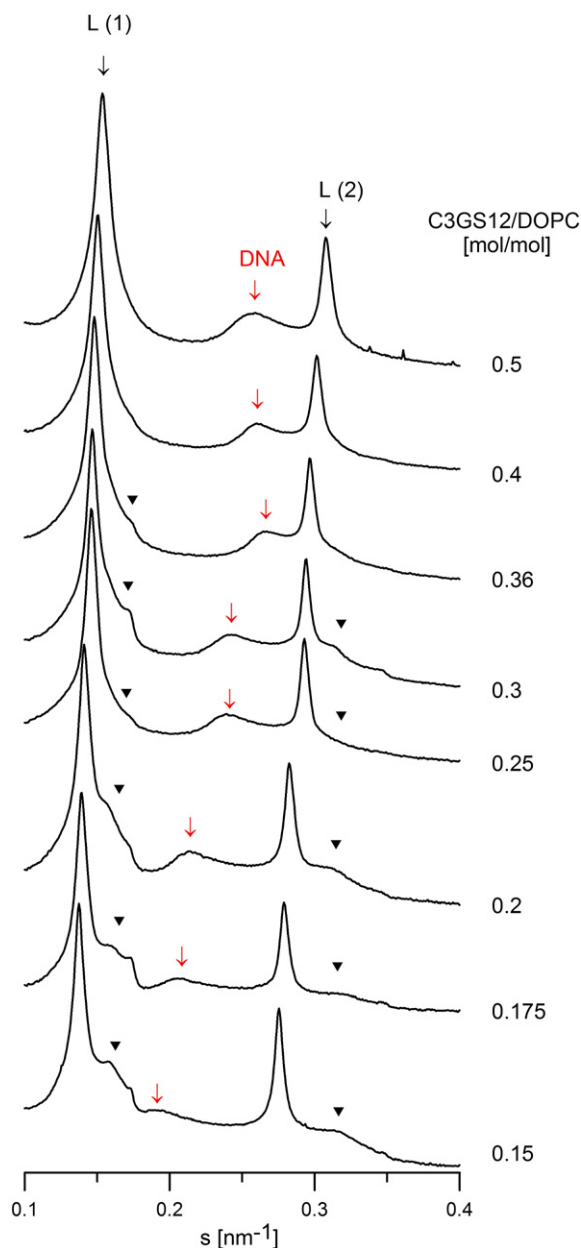


Fig. 2. SAXD patterns of C3GS12-DOPC-CTDNA complexes at ionic strength of 150 mM NaCl solution (20 °C). Bold triangles mark 1st and 2nd order reflections of  $L_B$  phases. Intensity [relative units] is in logarithmic scale.

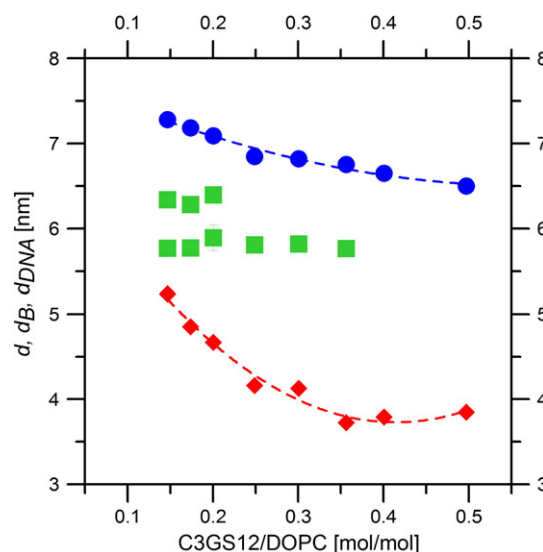


Fig. 3. Dependence of structural parameters  $d$  (●),  $d_B$  (■) and  $d_{DNA}$  (◆) [nm] of C3GS12-DOPC-CTDNA complexes on the molar ratio C3GS12/DOPC (150 mM NaCl, 20 °C). Dashed lines are only guidelines. Error bars smaller than the symbols are not shown.

6.5 nm. The decrease of  $d$  is typical for lamellar systems with incorporated surfactant molecules. The shorter alkyl tails of surfactant and charged head groups induce the changes in the hydrophobic as well as the hydrophilic regions of the bilayer, both leading to a decrease of bilayer thickness and repeat distance  $d$ . The described changes of lipid bilayer can be well explained with the “free volume” model [36–38]. According to this model the shorter tails of incorporated molecules induce a higher incidence of *gauche*-conformation of lipid tails. This effect together with lateral expansion of the bilayer leads to the decrease of bilayer thickness. Beside the periodicity of  $L_\alpha^c$  phase, the ratio C3GS12/DOPC affects the arrangement of DNA strands. The interhelical distance  $d_{DNA}$  as a function of the molar ratio C3GS12/DOPC displays a nonlinear decreasing tendency from 5.24 nm at the ratio 0.15 to 3.72 nm at the ratio 0.36. In the range  $0.36 \leq \text{C3GS12/DOPC} \leq 0.5$  the  $d_{DNA}$  did not change significantly and a “plateau” of  $d_{DNA}$  is observed. The higher amount of surfactant in the mixture is accompanied with a tighter arrangement of parallel DNA strands [3]. Usually, the molar ratio of cationic to neutral content is related to the parameter called surface charge density of CLs [4,39]. The surface charge density (cationic charge/lipid membrane area) is considered as the governing parameter for the  $d_{DNA}$  in the charge-neutral complexes, on the assumption of complete counterions release. Despite the tight relation between  $d_{DNA}$  and surface charge density, the dependence of  $d_{DNA}$  on the C3GS12/DOPC displays a non-linear behavior. This could be caused by the presence of additional  $L_B$  phase in the sample. The  $L_B$  phases have the periodicity  $d_B \sim 5.9$ –6.4 nm and do not change significantly in the studied range of the molar ratios C3GS12/DOPC.

### 3.1.2. C2GS12-DOPC-CTDNA complexes at various ionic strengths

To unravel the role of surface charge density and ionic strength on the structure of DNA-CLs complexes, we prepared the series of samples with C2GS12 in the same manner of stepwise addition of CTDNA solution at various constant ratios C2GS12/DOPC = 0.15, 0.2, 0.3, 0.5 mol/mol, and at concentrations of NaCl in the range 5–200 mM. Selected SAXD patterns are shown in Fig. 4A–C. All reported diffraction patterns show a condensed lamellar phase  $L_\alpha^c$ , the position of the reflection due to DNA–DNA correlation is marked by a red arrow. In addition to  $L_\alpha^c$  phase one can recognize other small peaks present in some diffractograms, which are marked by a full triangle. We identified them as the lamellar phase  $L_B$ . At C2GS12/DOPC = 0.3 and ionic strength corresponding to 5 mM NaCl only the  $L_\alpha^c$  phase is formed. At increased concentration of NaCl (50, 150, 200 mM),  $L_B$  phase is apparent together



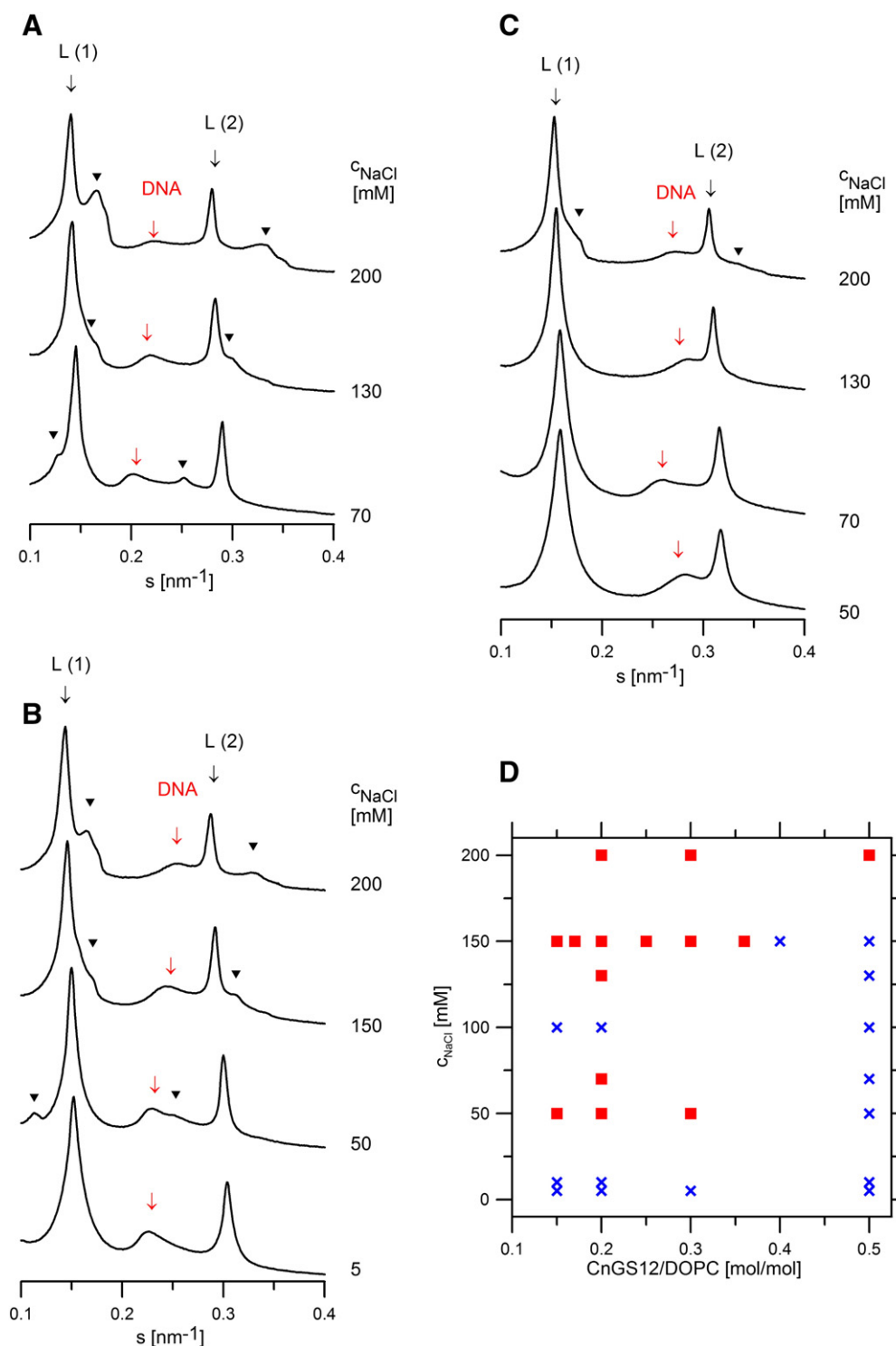


**Fig. 4.** (A)–(C) SAXD patterns of C2GS12-DOPC-CTDNA complexes at various concentration of NaCl bulk solution (20 °C); (A) C2GS12/DOPC = 0.2; (B) 0.3; (C) 0.5 mol/mol. Bold triangles mark 1st and 2nd order reflections of  $L_B$  phases. Intensity [relative units] is in logarithmic scale. (D) Occurrence of phase coexistence in CnGS12-DOPC-DNA complexes as a function of CnGS12/DOPC molar ratio and concentration of NaCl; (■) the samples where the phase coexistence was identified, (X) only  $L_\alpha^C$  phase was detected in the sample.

with  $L_\alpha^C$  phase. The increased ionic strength and the low surface charge density cause a higher intensity of  $L_B$  phase's reflections and a shift of the  $L_B$  phase's reflection position. It should be stressed that the samples prepared at C2GS12/DOPC = 0.5 mol/mol kept pure  $L_\alpha^C$  phase up to the ionic strength 200 mM NaCl, where the phase coexistence occurred. These results are in accordance with the ones obtained with previous series of C3GS12-DOPC-DNA samples and support the observation that lower molar ratio CnGS12/DOPC and increased ionic strength coincide

with the phase coexistence. The presence of phase coexistence in all studied CnGS12-DOPC-DNA complexes is schematically illustrated in Fig. 4D. At 50 mM  $\leq$  NaCl concentration  $\leq$  150 mM, the phase coexistence was detected in complexes at molar ratios CnGS12/DOPC  $\leq$  0.3 mol/mol, with exception of those prepared at  $C_{NaCl}$  = 100 mM (discussed below). The structural parameters of  $L_\alpha^C$  and  $L_B$  phases at C2GS12/DOPC = 0.2 mol/mol are shown in Fig. 5A. For  $L_\alpha^C$ , the repeat distance  $d$  slightly increases and  $d_{DNA}$  decreases with increasing ionic

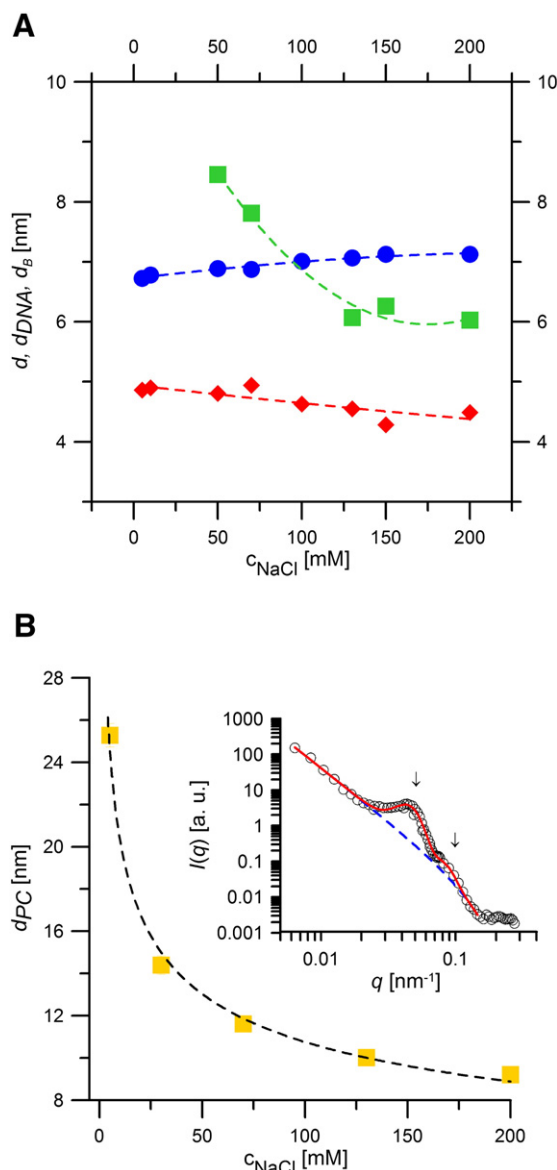


**Fig. 5.** (A) Dependence of structural parameters  $d$  (●),  $d_{DNA}$  (◆) and  $d_B$  (■) at 20 °C; C2GS12/DOPC = 0.2 mol/mol. Dashed lines are only guidelines. Error bars smaller than the symbols are not shown. (B) The dependence of  $d_{PC}$  of non-extruded liposome dispersion at C2GS12/DOPC = 0.2 mol/mol on the NaCl concentration of bulk solution; dashed line is only guideline. Error bars smaller than the symbols are not shown. Inset: SANS intensity of non-extruded liposome dispersion at C2GS12/DOPC = 0.2 mol/mol in 30 mM NaCl; arrows mark the 1st and 2nd order correlation peaks due to multilamellar structure. Dashed line represents the Guinier approximation, full line the fit by Eq. (4), supplementary material.

strength. The repeat distance  $d_B$  of  $L_B$  phase shows strong non-linear dependence on the ionic strength of the solution. We observe its decrease from  $d_B \sim 8.5$  nm at 50 mM NaCl up to  $d_B \sim 6$  nm at 200 mM NaCl. Note that the expected  $d_B$  at 100 mM NaCl should be very similar to  $d$  of  $L_\alpha$  phase, and thus both phases would be difficult to discriminate in SAXD patterns. While the effect of ionic strength is significant in the complexes with low surface charge density, the complexes at C2GS12/DOPC = 0.5 show the phase coexistence only at the highest ionic strength of  $c_{NaCl} = 200$  mM, showing  $d_B \sim 5.7$  nm.

### 3.1.3. Small angle neutron scattering

We employed SANS experiments to examine the structural composition of cationic liposome dispersion without the presence of DNA at various ionic strength of NaCl bulk solutions. Generally, when the surface charge density of lipid membrane is higher than  $1\text{--}2 \mu\text{C}/\text{cm}^2$ ,

unilamellar vesicles are formed [40]. Supposing the surface area per 1 lipid molecule approximately  $0.7 \text{ nm}^2$  and per one C2GS12 molecule approximately  $0.79 \text{ nm}^2$  [41], one can easily calculate that the surface charge density of our mixture C2GS12/DOPC = 0.2 mol/mol fulfills the criterion. However, dynamic light scattering measurements revealed a big difference in the particle size of our C2GS12/DOPC mixture as a function of ionic strength (see Section 2.2. Preparation of cationic liposomes). To investigate the structural properties and to test the presence of multiple phases within the liposome dispersions, we have chosen a representative dispersion having low molar ratio C2GS12/DOPC = 0.2 and forming the  $L_B$  phase in DNA-CLs complexes. The inset in Fig. 5B shows the SANS curve of C2GS12/DOPC = 0.2 mol/mol liposomes prepared at 30 mM NaCl. Actually, the SANS curves of all tested liposomes have shown 1–2 correlation peaks superposed on the scattering curve from unilamellar liposomes. The correlation peaks are a consequence of a lamellar phase occurring in the mixture, i.e. oligolamellar or multilamellar vesicles. With the aim to compare the repeat period  $d_B$  of  $L_B$  phases with characteristics of liposome dispersions, we extracted the observed intensity maxima from SANS curves according to [34], for more details see the Supplementary material. The position of 1st order correlation peak's maximum was used to calculate the repeat distance  $d_{PC}$  in C2GS12/DOPC liposome dispersion. The plot of  $d_{PC}$  as a function of NaCl concentration is shown in Fig. 5B. We observe the decreasing of  $d_{PC}$  in dependence on the NaCl concentration. The  $d_{PC}$  decreases from  $\sim 25.3$  nm at 5 mM NaCl down to  $\sim 9.2$  nm at 200 mM NaCl. SANS experiments confirmed that the studied liposome dispersions contain the lamellar arrangement of lipid bilayers giving one repeat distance  $d_{PC}$ . When comparing  $d_{PC}$  of liposomes C2GS12-DOPC and  $d_B$  of  $L_B$  phase in C2GS12-DOPC-DNA complexes ( $d_B \sim 8.8\text{--}5.7$  nm at 50–200 mM NaCl), one can see a marked shift in the repeat distance towards the smaller values in the case of  $L_B$  phase. The repeat period of  $L_B$  phase does not correspond to the repeat period of CLs obtained by SANS. The high ionic strength of bulk solution partially screens the surface charge of lipid bilayers and as a result, the mutual repulsion of lipid bilayers weakens and  $d_{PC}$  decreases with NaCl concentration increase. Such dramatic change in the repeat distance due to the ionic strength charge screening was documented in literature for calcium binding to dipalmitoylphosphatidylcholine (DPPC) bilayers [42,43]. We observed similar effect studying the DNA interaction with DPPC in the presence of  $\text{Zn}^{2+}$  [34], when due to macroscopic phase separation in the sample, DPPC +  $\text{Zn}^{2+}$  has shown the decrease in the periodicity  $\sim$ from 20 to 7 nm with increasing ionic strength from 35 to 330 mM.

### 3.1.4. CnGS12-DOPC-DNA samples prepared by one step addition of DNA

With the aim to test our experimental protocol, we prepared the series of samples using the method of one-step addition of DNA solution to liposome dispersion. The samples contained CnGS12 with  $n = 2\text{--}4$  ( $n$  is the number of spacer carbons) at ratio CnGS12/DOPC = 0.2 mol/mol. The ionic strength of bulk solution corresponded to 150 mM NaCl solution. The SAXD patterns of these samples are shown in Fig. 6. The positions of well resolved reflections confirmed the presence of  $L_\alpha^C$  phase in all samples. We did not observe any indications of phase coexistence in diffraction patterns, contrary to samples described above which were prepared under basically the same conditions, except for the method of addition of DNA solution. For small numbers of spacer carbons in the range  $n = 2\text{--}4$ , the lamellar periodicity  $d$  did not change significantly and the value  $d \sim 7.1$  nm was extracted. This shows unequivocally that the method of complex preparation plays an important role in the process of DNA-CLs interaction, together with other physico-chemical conditions.

### 3.2. ITC measurements

The samples for SAXD experiments, as mentioned above, were prepared at constant molar ratio DNA/CnGS12 = 1 mol bp/mol. Because some of the samples exhibited the presence of additional lipid

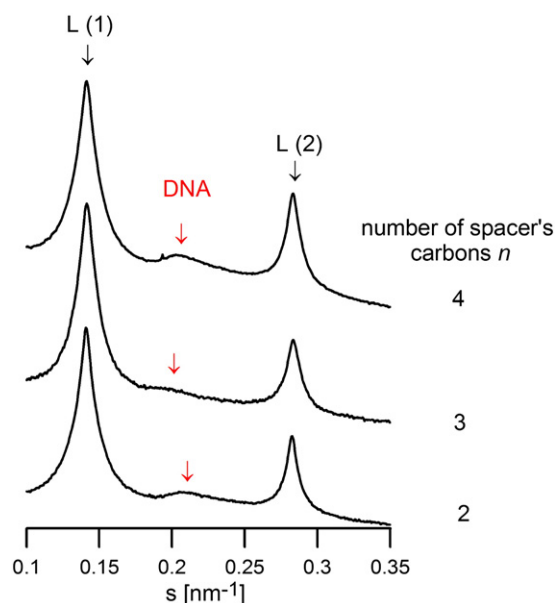


**Fig. 6.** SAXD patterns of CnGS12-DOPC-CTDNA complexes at ionic strength of 150 mM NaCl solution (20 °C). CnGS12/DOPC = 0.2 mol/mol, intensity [relative units] is in logarithmic scale.

phases  $L_B$  in SAXD patterns, we performed ITC measurement to reveal if the complexes at calculated isoelectric point DNA/CnGS12 = 1 mol bp/mol could contain redundant cationic liposomes at high ionic strength of bulk solution. ITC enables to observe the process of interaction throughout the wide range of DNA/C2GS12 ratios and at different concentration of NaCl in the bulk solution. CLs for ITC measurements were prepared at molar ratio C2GS12/DOPC = 0.2 mol/mol. Representative parts of thermograms obtained in 5 mM and 150 mM NaCl solution are shown in Fig. 7. The stepwise addition of HTDNA solution into the liposome dispersion placed in the titration cell resulted in an endothermic process. After a certain number of injections, continuing addition of HTDNA shows up as small and constant exothermic changes, arising from the dilution of HTDNA solution. The average of these final peaks was taken as the dilution heat effect, and used to correct the observed heat effects during the reaction, as explained above. For each titration, the reaction endpoint was estimated as the molar ratio DNA/C2GS12 [mol bp/mol], where the last endothermic peak is observed. Beyond this ratio further addition of DNA did not lead to the condensation, as shown by the absence of endothermic peaks. The complex formation is thus considered to be finished at this point. At low ionic strength, we observed several endothermic peaks, of rather constant area, which decrease fast to close to zero, and become negative in the last injections. At high ionic strength the number of endothermic peaks is very much reduced and their areas are smaller than the ones observed at low ionic strength. The inset in Fig. 7 shows the plot of the obtained  $Q$  in dependence on the ratio DNA/C2GS12. The reaction endpoint as well as the calorimetric parameter  $\Delta H$  [kJ/mol bp] was calculated as average from the values obtained in at least two independent experiments (Table 1). The “titration endpoint”, i.e., the ratio at which the condensation (interaction) can be considered to have finished, occurred at DNA/C2GS12 = 0.52 mol bp/mol at 5 mM NaCl and at a considerably lower ratio DNA/C2GS12 = 0.11 mol bp/mol at ionic strength of 150 mM NaCl. The  $\Delta H$  of the DNA-CLs interaction at 5 mM NaCl is  $15.1 \pm 0.2$  kJ/mol bp, a value that is in agreement with the one reported in a previously published paper, where the vesicles of pure gemini surfactants C2GS18:1 (18-carbon chain with one double bond) or of mixtures of C3GS18:1/DOPE were titrated with DNA in 10 mM NaBr. The reported  $\Delta H$  was in the range 10–15 kJ/mol bp in the initial phase of DNA

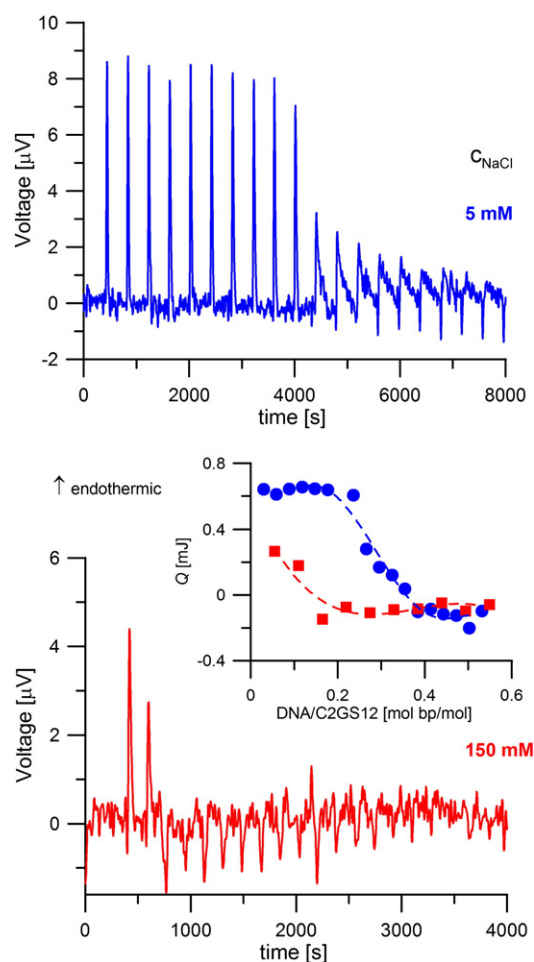


**Fig. 7.** Representative parts of thermograms obtained by the titration of C2GS12-DOPC liposome dispersion with HTDNA in 5 mM NaCl and 150 mM NaCl. Inset: Profile of heat  $Q$  [mJ] vs. ratio DNA/C2GS12 [mol bp/mol] obtained by titration of C2GS12-DOPC liposome dispersion with HTDNA in 5 mM NaCl (●) and 150 mM NaCl (■).

condensation [18]. The  $\Delta H = 15.1$  kJ/mol bp observed in our experiments at low ionic strength (5 mM NaCl) differs significantly from that obtained at 150 mM NaCl,  $4.7 \pm 0.1$  kJ/mol bp. The principally similar results were obtained even at the NaCl concentration 70 mM (Table 1). The endothermic character of the DNA-CLs interaction was observed with different cationic lipids and surfactants [6,44]. A shift of the endpoints to higher ratios CLs/DNA was observed at increased ionic strength [5,6,45]. The complex formation can be considered to involve the following partial processes: i) electrostatic attraction between DNA and cationic liposomes [46]; ii) release of counterions and bound water in hydration layer [47–49] iii) complete remodeling of the structure of the complexes [50]. The observed endothermic enthalpy indicates that the interaction is driven by the increase in entropy due to the release of bound counterions and water from the surface of DNA and CLs. It has been shown that increasing ionic strength reduces the amount of DNA binding within the complex, as arises from our finding of a much smaller number of peaks observed at higher ionic strengths. The shift of the reaction endpoint to the lower molar ratio DNA/C2GS12 = 0.1 mol bp/mol in 150 mM NaCl indicates that samples prepared at calculated isoelectric point could contain a relative excess of DNA, but not of cationic liposomes.

### 3.3. Zeta potential measurements

Zeta potential ( $\zeta$  potential) measurements were performed with the aim to confirm the ITC results and to study the changes of electric

**Table 1**  
Calorimetric enthalpies, titration endpoints as obtained by ITC measurements and isoelectric points obtained from  $\zeta$  potential measurements of C2GS12-DOPC-HTDNA complexes.

Concentration of NaCl [mM]	Ratio C2GS12/DOPC [mol/mol]	$\Delta H$ [kJ/mol bp]	Titration endpoint DNA/C2GS12 [mol bp/mol]	Isoelectric point DNA/C2GS12 [mol bp/mol]	Zeta potential at titration endpoint [mV]
5	0.2	$15.1 \pm 0.2$	$0.52 \pm 0.22$	$0.543 \pm 0.006$	$9.3 \pm 5$
	0.3				
70	0.2	$5.4 \pm 0.8$	$0.100 \pm 0.001$	$0.175 \pm 0.003$	$19.7 \pm 5$
	0.3				
150	0.2	$4.7 \pm 0.1$	$0.110 \pm 0.001$		

potential of particles prepared by additions of DNA solution to CLs. We used the liposomes prepared as described above composed from the mixture C2GS12/DOPC at ratio 0.3 mol/mol at ionic strength corresponding to 5 mM NaCl and 70 mM NaCl. After the addition of DNA to CLs and short mixing, the DNA-CLs were transferred into the U-tube measurement cell a few minutes after preparation. The dependence of  $\zeta$  potential vs. DNA/C2GS12 ratio is shown in Fig. 8. We fitted the linear parts of the dependences and approximated the isoelectric point as the ratio where the  $\zeta$  potential values cross zero. The starting  $\zeta$  potential of liposome dispersions without DNA addition is approximately +80 mV at 5 mM NaCl and approximately +40 mV at 70 mM NaCl. The  $\zeta$  potential of complexes after crossing the isoelectric point reaches the values in the range from –30 to –40 mV. The average isoelectric points calculated from two independent measurements are listed in Table 1. At 5 mM NaCl, the ratio of DNA/C2GS12 where the  $\zeta$  potential reached zero is about 0.54 mol bp/mol. The increased ionic strength of 70 mM NaCl considerably shifted the ratio DNA/C2GS12 towards a lower value, about 0.175 mol bp/mol. In principle, the  $\zeta$  potential results are consistent with ITC. A small difference between titration endpoint and isoelectric point occurs at 70 mM NaCl, what can be caused by a slightly different surface charge density of CLs used in experiments. In fact, the titration endpoint at 5 mM NaCl corresponds to  $\zeta$  potential +9.3 mV and at 70 mM NaCl to +19.7 mV. In terms of the reaction finish indication, the values of titration endpoint and  $\zeta$  potential are in good agreement at 5 mM NaCl, where  $\zeta$  potential +9.3 mV represents only a small fraction of initial  $\zeta$  potential value. The increased ionic strength partially screens the surface charge and promotes the precipitation, which occurs much earlier in comparison with what was observed at low ionic strength. Additions of DNA to CLs upon the isoelectric point lead to the

formation of particles with negative  $\zeta$  potential, but did not induce the endothermic heat change detectable by ITC. This behavior suggests that DNA-CLs complexes formed at calculated isoelectric point (based on nominal charges) carry in fact negative charge at low as well as high ionic strength. The high ionic strength reduces the initial  $\zeta$  potential of CLs. The isoelectric point is reached at smaller ratio DNA/C2GS12 in comparison with the calculated.

#### 4. Discussion

SAXD measurements of CnGS12-DOPC-DNA complexes confirmed the  $L_\alpha$  phase or the coexistence of  $L_\alpha$  and  $L_B$  phase in complexes.  $L_B$  phase appears in dependence on the low surface charge density and increased ionic strength (corresponding to 50, 70, 130, 150, 200 mM NaCl solution). The  $L_B$  was identified as a lamellar phase with periodicity in the range 8.5–6 nm at the various CnGS12/DOPC ratios tested. The periodicity and the behavior of  $L_B$  in C2GS12-DOPC-DNA complexes suggest that  $L_B$  does not correspond to pure DOPC. We assume that  $L_B$  phase contains CnGS12 as well as DOPC. The uncompensated charge of the part of the system showing  $L_B$  phase leads to the electrostatic repulsion between lipid bilayers, which is more pronounced at small ionic strength and is partially screened at higher ionic strength.

Koltover et al. [3] have reported that the lamellar complexes containing cationic lipid dioleoyltrimethylammonium propane (DOTAP) and DOPC exhibited an additional phase at the weight fraction of DOPC = 0.85, corresponding to the molar ratio DOTAP/DOPC = 0.18. The additional phase with the periodicity 7.65 nm was ascribed to the partial demixing of the lipid components. The authors investigated also the influence of high ionic strength on the structure of DNA-DOTAP-DOPC complexes. They observed that  $d_{DNA}$  increases with increasing ionic strength, contrary to our samples (Fig. 5A). When the ionic strength started to be too high with respect to surface charge density of CLs, it screened the counterion-release mechanism, resulting in rapid decrease of  $d_{DNA}$  and increase of  $d$ . Ultimately the regular structure of complexes completely desintegrated. Microscopic phase segregation was reported also in DNA-CLs complexes based on dilauroylphosphatidylcholine/gemini surfactant C4GS12. The complexes showed formation of micro-domains enriched in C4GS12 for samples of molar ratio C4GS12/dilauroylphosphatidylcholine  $\geq 0.35$  [51]. The presence of multiple phases was observed in aza- and imino-substituted plasmid-gemini surfactant-DOPE nanoparticles using SAXD [52]. DNA-induced lipid segregation in DNA-CLs complexes was also detected using differential scanning calorimetry (DSC) [23,53], fluorescence measurements [54] and nuclear magnetic resonance [22]. The phenomena of lateral phase segregation have been observed frequently also in complexes formed between DNA and zwitterionic phospholipids in the presence of divalent cations [55–57].

In addition to the observation of coexisting phases within one structure that cannot be separated macroscopically, bulk macroscopic phase separation can also occur. SAXD cannot discriminate between the coexistence of two phases that are either macroscopically separated but both present within the studied volume of a sample or that coexist within one structure. Thorough investigation of the obtained periodicities, as well as microscopic investigation and inspection of the sample mixture can help to identify the structure present. Actually,

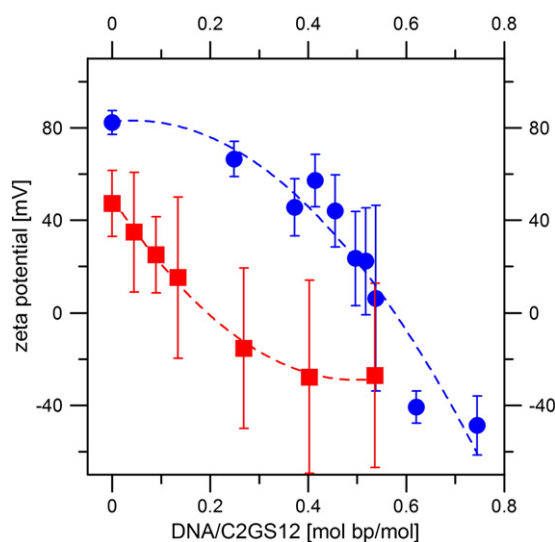


**Fig. 8.** Profile of  $\zeta$  potential vs. ratio DNA/C2GS12 [mol bp/mol] of complexes C2GS12-DOPC-HTDNA in 5 mM NaCl (●) and 70 mM NaCl (■); (C2GS12/DOPC = 0.3 mol/mol). Dashed lines are only guidelines.



we have observed such macroscopic phase separation in a mixture DNA/DPPC/Zn<sup>2+</sup> [34] when low Zn<sup>2+</sup> concentrations (<20 mM) support the formation of DNA + DPPC + Zn<sup>2+</sup> complexes, however a bulk phase separation of DPPC + Zn<sup>2+</sup> and DNA + DPPC + Zn<sup>2+</sup> was observed at high ionic strength of solution. With the aim to discriminate the character of phase coexistence in our samples, we investigated the C2GS12-DOPC dispersion without DNA by means of small angle neutron scattering. The results suggested that the phase coexistence observed by SAXD in DNA-CLs complexes has the origin in the microscopic phase segregation rather than the presence of primary C2GS12-DOPC dispersion in the sample.  $L_B$  phase is “trapped” in the complex and represents a mixture of DOPC and CnGS12 with uncompensated surface charge. The shift in repeat distances  $d_B$  and  $d_{PC}$  can be caused by different effective surface charge density of the  $L_B$  phase in comparison with the primary DOPC/CnGS12 mixture. The change in effective surface charge density could have its origin in a lateral diffusion of CnGS12 molecules leading to the formation of DOPC-rich and CnGS12-rich domains within the membrane. CnGS12 rich domains are attracted by DNA polyanion forming the  $L_\alpha^c$  phase. Moreover the ITC and  $\xi$  potential have proven that the samples prepared at calculated isoelectric point contain an excess of DNA. High ionic strength forces the early precipitation of lipid even with relatively small amount of DNA. Thus we suppose that the presence of macroscopically separated CLs dispersion in samples for SAXD is improbable.

The excess of solved DNA in terms of effective charge in samples for SAXD could osmotically stress the bilayers and affect the repeat distance. However, the maximum concentration of free DNA in SAXD samples could be ~1 g/l in the hypothetical case of no interaction with CLs. This concentration is low and its osmotic effect in comparison to that induced by NaCl solution is negligible [58]. The stepwise addition of DNA into the CnGS12-DOPC bilayers with low surface charge density and the lateral diffusion of molecules in the fluid membrane are most probably the factors responsible for the observed phase coexistence.

The set of samples prepared by the one step addition of DNA to the liposome dispersion did not show the phase coexistence. The SAXD data confirmed the presence of  $L_\alpha^c$  phase in the complexes, without the presence of  $L_B$  phase. These findings indicate that the method of preparation is one of the factors affecting the possibility for phase coexistence to occur. The lateral segregation of cationic components occurring during the interaction with DNA reported has been already mentioned in literature. High ionic strength partially screens the surface charge of CLs as has been shown by  $\xi$  potential measurement. Both ITC and  $\xi$  potential measurements have proven the decreased ability of CLs to bind DNA at high ionic strength. The interaction of DNA with CLs requires at least a critical surface charge density of the lipid membrane surface, which strongly depends on ionic strength of bulk solution [59]. The two methods of DNA-CLs complexes preparation used in our study led to a structural variability of complexes. The first addition of DNA solution to CLs results in a DNA complexation accompanied with a partial segregation of cationic surfactant and DOPC at high ionic strength. The accumulated surfactants increase the surface charge of domain and effectively bind DNA. Continuing DNA addition produce next lipid segregation until a moment, when the surface charge density of the DNA-free lipid membrane decreases under a critical value. Thus further added DNA does not interact with CLs, especially at conditions of high ionic strength, where higher surface charge density is required. The remaining surfactant - depleted lipid fraction manifested itself as a coexisting phase with repeat period  $d_B$  differing from the pure DOPC as well as from the initial mixture of CLs. This suggestion supports also the changes of  $d_{DNA}$  observed with increasing ionic strength. Despite the high ionic strength attenuates the DNA-CLs interaction,  $d_{DNA}$  slightly decreases with increasing NaCl concentration, indicating the tighter packing of DNA strands. The decrease of  $d_{DNA}$  indicates the increased surface charge density at higher ionic strength. The one-step addition of DNA does not allow the processing of the gradual lipid demixing in the membrane as has been proposed above. The aggregation due to electrostatic

DNA – cationic liposomes interaction is a fast process [50] and both DNA and liposomes undergo a complete topological transformation. Entropically driven DNA-CLs interaction facilitate the creation of complexes, which are not necessarily isoelectric, and fast precipitation forms stable dense colloidal particles. We can consider the one-step addition of DNA to be an appropriate method for complex preparation because it enables the effective utilization of used components meanwhile the DNA-CLs complex is forming.

The reaction endpoint in 5 mM NaCl obtained by ITC corresponds to the isoelectric point evaluated using  $\xi$  potential measurements. The actual isoelectric point was detected at approximately two times lower ratio DNA/C2GS12 than the calculated isoelectric point. It has been reported that  $\zeta$  potential did not necessarily cross the zero at the calculated isoelectric point [3,18,19,60], and that the  $\zeta$  potential of complexes formed in water was significantly affected by the addition of NaCl [20]. Results published in literature indicate that for gemini surfactants with a short spacer, the spacing between the two positive charges is so small that the surfactant acts like a divalent cationic surfactant [61]. However, CLs represent more complex system than surfactants in micelle or in monomeric form. At low surface charge density, the two interconnected cationic moieties of CnGS12 having a small distance seem to interact as a single point charge in terms of lipid membrane's interaction with DNA. However, DNA condensation efficiency decreases with decreasing cationic surfactant/lipid ratio [39]. Thus the low surface charge density of CLs used in this study can be responsible for the deviations from a simple electrostatic binding of CnGS12 and DNA.

## 5. Conclusions

CLs based on the gemini surfactant of type CnGS12 and the helper lipid DOPC condense the DNA even at high ionic strength and low surface charge density, giving rise to regularly structured complexes. SAXD measurements revealed the presence of the  $L_\alpha^c$  phase in all studied CnGS12-DOPC-DNA. The  $d_{DNA}$  parameter characterizing the distance between adjacent DNA strands depends on the surface charge density. The high ionic strength, the process of complex preparation and the low fraction of surfactant in the lipid mixture coincide with the phase coexistence in the samples. The titration endpoint of the DNA-CLs interaction as well as the isoelectric point of the complexes formed was found at DNA/CnGS12 ~0.5 mol bp/mol in 5 mM NaCl bulk solution. High ionic strength (150 mM) shifted the titration endpoint to the ratio DNA/CnGS12 ~0.1 mol bp/mol. The  $\zeta$  potential in 70 mM NaCl crossed the zero at DNA/CnGS12 ~0.175 mol bp/mol. The amount of DNA bound in the complexes can be varied depending on the process of sample preparation and on solution conditions. We suppose that the phase coexistence has the origin in the lipid phase segregation promoted by composition of CLs, ionic strength of bulk solution and the process of sample preparation. The all are factors leading either to the weakening of DNA-CLs interaction, or to the unequal ratio of DNA and CLs during the first phase of complex formation. Some published works bring evidence for the lipid lateral phase segregation as a result of changed thermodynamic conditions, such as temperature or ionic strength. One of the strong factors that trigger lateral phase separation is the interaction of charged membranes with oppositely charged macromolecules or ions. In that case two lipid phases coexist, the charged component-enrich fraction binding the oppositely charged molecule and charge component-depleted fraction does not bind [62]. Our experiments and the novel findings therein provide wealth of information for preparation protocol's optimization.

## Acknowledgements

Authors thank Prof. P. Balgavý for the fruitful discussion and his help on the manuscript preparation. Financial support provided by the European Community's Seventh Framework Program (FP7/2007–2013) under grant agreement no. 226716 (HASYLAB project I-20090216

EC), by the JINR project 07-4-1069-09/2011, by the VEGA grant 1/0292/09 to DU, by SAIA, n. o. to PP, and by FCT through CIQ(UP) is gratefully acknowledged. MB and PP would like to thank Prof. Baltazar Castro's group for the access to the nanoZetasizer instrument.

## Appendix A. Supplementary data

Supplementary data to this article can be found online at [doi:10.1016/j.bpc.2011.09.002](https://doi.org/10.1016/j.bpc.2011.09.002).

## References

- [1] P.L. Felgner, T.R. Gadek, M. Holm, R. Roman, H.W. Chan, M. Wenz, J.P. Northrop, G.M. Ringold, M. Danielsen, Lipofection: a highly efficient, lipid-mediated DNA-transfection procedure, *Proceedings of the National Academy of Sciences of the United States of America* 84 (1987) 7413–7417.
- [2] T. Salditt, I. Koltover, J.O. Rädler, C.R. Safinya, Two-dimensional smectic ordering of linear DNA chains in self-assembled DNA-cationic liposome mixtures, *Physical Review Letters* 79 (1997) 2582–2585.
- [3] I. Koltover, T. Salditt, C.R. Safinya, Phase diagram, stability, and overcharging of lamellar cationic lipid-DNA self-assembled complexes, *Biophysical Journal* 77 (1999) 915–924.
- [4] A.J. Lin, N.L. Slack, A. Ahmad, C.X. George, C.E. Samuel, C.R. Safinya, Three-dimensional imaging of lipid gene-carriers: membrane charge density controls universal transfection behavior in lamellar cationic liposome-DNA complexes, *Biophysical Journal* 84 (2003) 3307–3316.
- [5] M.T. Kennedy, E.V. Pozharski, V.A. Rakhmanova, R.C. MacDonald, Factors governing the assembly of cationic phospholipid-DNA complexes, *Biophysical Journal* 78 (2000) 1620–1633.
- [6] E. Pozharski, R.C. MacDonald, Thermodynamics of cationic lipid-DNA complex formation as studied by isothermal titration calorimetry, *Biophysical Journal* 83 (2002) 556–565.
- [7] D. Hirsch-Lerner, M. Zhang, H. Eliyahu, M.E. Ferrari, C.J. Wheeler, Y. Barenholz, Effect of “helper lipid” on lipoplex electrostatics, *Biochimica et Biophysica Acta Biomembranes* 1714 (2005) 71–84.
- [8] H. Farhood, N. Serbina, L. Huang, The role of dioleoyl phosphatidylethanolamine in cationic liposome-mediated gene-transfer, *Biochimica et Biophysica Acta Biomembranes* 1235 (1995) 289–295.
- [9] B.G. Tenchov, L. Wang, R. Koynova, R.C. MacDonald, Modulation of a membrane lipid lamellar-nonlamellar phase transition by cationic lipids: a measure for transfection efficiency, *Biochimica et Biophysica Acta Biomembranes* 1778 (2008) 2405–2412.
- [10] D.D. Lasic, H. Strey, M.C.A. Stuart, R. Podgornik, P.M. Frederik, The structure of DNA-liposome complexes, *Journal of the American Chemical Society* 119 (1997) 832–833.
- [11] J.O. Rädler, I. Koltover, T. Salditt, C.R. Safinya, Structure of DNA-cationic liposome complexes: DNA intercalation in multilamellar membranes in distinct interhelical packing regimes, *Science* 275 (1997) 810–814.
- [12] I. Koltover, T. Salditt, J.O. Rädler, C.R. Safinya, An inverted hexagonal phase of cationic liposome-DNA complexes related to DNA release and delivery, *Science* 281 (1998) 78–81.
- [13] K.K. Ewert, H.M. Evans, A. Zidovska, N.F. Boussein, A. Ahmad, C.R. Safinya, A columnar phase of dendritic lipid-based cationic liposome-DNA complexes for gene delivery: hexagonally ordered cylindrical micelles embedded in a DNA honeycomb lattice, *Journal of the American Chemical Society* 128 (2006) 3998–4006.
- [14] A.J. Kirby, P. Camilleri, J.B.F.N. Engberts, M.C. Feiters, R.J.M. Nolte, O. Soderman, M. Bergsma, P.C. Bell, M.L. Fielden, C.L.G. Rodriguez, P. Guedat, A. Kremer, C. McGregor, C. Perrin, G. Ronsin, M.C.P. van Eijk, Gemini surfactants: new synthetic vectors for gene transfection, *Angewandte Chemie, International Edition* 42 (2003) 1448–1457.
- [15] F.M. Menger, C.A. Littau, Gemini surfactants: a new class of self-assembling molecules, *Journal of the American Chemical Society* 115 (1993) 10083–10090.
- [16] P. Camilleri, A. Kremer, A.J. Edwards, K.H. Jennings, O. Jenkins, I. Marshall, C. McGregor, W. Neville, S.Q. Rice, R.J. Smith, M.J. Wilkinson, A.J. Kirby, A novel class of cationic gemini surfactants showing efficient *in vitro* gene transfection properties, *Chemical Communications* (2000) 1253–1254.
- [17] I. Badea, R. Verrall, M. Baca-Estrada, S. Tikoo, A. Rosenberg, P. Kumar, M. Foldvari, *In vivo* cutaneous interferon-gamma gene delivery using novel dicationic (gemini) surfactant-plasmid complexes, *The Journal of Gene Medicine* 7 (2005) 1200–1204.
- [18] C. Wang, X. Li, S.D. Wettig, I. Badea, M. Foldvari, R.E. Verrall, Investigation of complexes formed by interaction of cationic gemini surfactants with deoxyribonucleic acid, *Physical Chemistry Chemical Physics* 9 (2007) 1616–1628.
- [19] B.A. Lobo, A. Davis, G. Koe, J.G. Smith, C.R. Middaugh, Isothermal titration calorimetric analysis of the interaction between cationic lipids and plasmid DNA, *Archives of Biochemistry and Biophysics* 386 (2001) 95–105.
- [20] K.K. Son, D.H. Patel, D. Tkach, A. Park, Cationic liposome and plasmid DNA complexes formed in serum-free medium under optimum transfection condition are negatively charged, *Biochimica et Biophysica Acta Biomembranes* 1466 (2000) 11–15.
- [21] K.K. Son, D. Tkach, K.J. Hall, Efficient *in vivo* gene delivery by the negatively charged complexes of cationic liposomes and plasmid DNA, *Biochimica et Biophysica Acta Biomembranes* 1468 (2000) 6–10.
- [22] C. Leal, D. Sandstrom, P. Nevsten, D. Topgaard, Local and translational dynamics in DNA-lipid assemblies monitored by solid-state and diffusion NMR, *Biochimica et Biophysica Acta Biomembranes* 1778 (2008) 214–228.
- [23] A. Michanek, N. Kristen, F. H. k. T. Nylander, E. Sparr, RNA and DNA interactions with zwitterionic and charged lipid membranes – a DSC and QCM-D study, *Biochimica et Biophysica Acta Biomembranes* 1798 (2010) 829–838.
- [24] D. Uhríková, A. Lengyel, M. Hanulová, S.S. Funari, P. Balgavý, The structural diversity of DNA-neutral phospholipids-divalent metal cations aggregates: a small-angle synchrotron X-ray diffraction study, *European Biophysics Journal with Biophysics Letters* 36 (2007) 363–375.
- [25] P. Mitrakos, P.M. Macdonald, DNA-induced lateral segregation of cationic amphiphiles in lipid bilayer membranes as detected via  $^2\text{H}$  NMR, *Biochemistry* 35 (1996) 16714–16722.
- [26] T. Imam, F. Devínský, I. Lacko, D. Mlynářčík, L. Krasnec, Preparation and antimicrobial activity of some new bisquaternary ammonium salts, *Die Pharmazie* 38 (1983) 308–310.
- [27] T.C. Huang, H. Toraya, T.N. Blanton, Y. Wu, X-ray powder diffraction analysis of silver behenate, a possible low-angle diffraction standard, *Journal of Applied Crystallography* 26 (1993) 180–184.
- [28] D. Chapman, The polymorphism of glycerides, *Chemical Reviews* 62 (1962) 433–453.
- [29] M. Kellens, W. Meeussen, H. Reynaers, Crystallization and phase-transition studies of tripalmitin, *Chemistry and Physics of Lipids* 55 (1990) 163–178.
- [30] C.M. Matos, J.L.C. Lima, S. Reis, A. Lopes, M. Bastos, Interaction of antiinflammatory drugs with EPC liposomes: calorimetric study in a broad concentration range, *Biophysical Journal* 86 (2004) 946–954.
- [31] L.E. Brigger, I. Wadso, Test and calibration processes for microcalorimeters, with special reference to heat conduction instruments used with aqueous systems, *Journal of Biochemical and Biophysical Methods* 22 (2002) 101–118.
- [32] M. Bastos, S. Hagg, P. Lonnbro, I. Wadso, Fast titration experiments using heat conduction microcalorimeters, *Journal of Biochemical and Biophysical Methods* 23 (1991) 255–258.
- [33] N. Kučerka, D. Uhríková, J. Teixeira, P. Balgavý, Thickness of the phospholipid bilayer in unilamellar liposomes: small-angle neutron scattering using contrast variation, *Biophysical Journal* 86 (2004) 379A.
- [34] D. Uhríková, P. Pullmannová, M. Bastos, S.S. Funari, J. Teixeira, Interaction of short fragmented DNA with dipalmitoylphosphatidylcholine bilayers in presence of zinc, *General Physiology and Biophysics* 28 (2009) 146–159.
- [35] M. Foldvari, I. Badea, S. Wettig, R. Verrall, M. Bagonluri, Structural characterization of novel gemini non-viral DNA delivery systems for cutaneous gene therapy, *Journal of Experimental Nanoscience* 1 (2006) 165–176.
- [36] P. Balgavý, F. Devínský, Cut-off effects in biological activities of surfactants, *Advances in Colloid and Interface Science* 66 (1996) 23–63.
- [37] T.X. Xiang, A computer simulation of free-volume distributions and related structural properties in a model lipid bilayer, *Biophysical Journal* 65 (1993) 1108–1120.
- [38] M.D. King, D. Marsh, Free volume model for lipid lateral diffusion coefficients. Assessment of the temperature dependence in phosphatidylcholine and phosphatidylethanolamine bilayers, *Biochimica et Biophysica Acta Biomembranes* 862 (1986) 231–234.
- [39] S.J. Ryhanen, M.J. Saily, T. Pauku, S. Borocci, G. Mancini, J.M. Holopainen, P.K.J. Kinnunen, Surface charge density determines the efficiency of cationic gemini surfactant based lipofection, *Biophysical Journal* 84 (2003) 578–587.
- [40] H. Hauser, Phospholipid vesicles, in: G. Cevc (Ed.), *Phospholipid Handbook*, Marcel Dekker Inc., New York, 1993, pp. 603–637.
- [41] S.D. Wettig, R.E. Verrall, Thermodynamic studies of aqueous m-s-m gemini surfactant systems, *Journal of Colloid and Interface Science* 235 (2001) 310–316.
- [42] Y. Inoko, T. Yamaguchi, K. Furuya, T. Mitsui, Effects of cations on dipalmitoyl phosphatidylcholine/cholesterol/water systems, *Biochimica et Biophysica Acta* 413 (1975) 24–32.
- [43] N.L. Yamada, H. Seto, T. Takeda, M. Nagao, Y. Kawabata, K. Inoue, SAXS, SANS and NSE Studies on “Unbound State” in DPPC/Water/ $\text{CaCl}_2$  System, *Journal of the Physical Society of Japan* 74 (2005) 2853–2859.
- [44] E. Gonçalves, R.J. Debs, T.D. Heath, The effect of liposome size on the final lipid/DNA ratio of cationic lipoplexes, *Biophysical Journal* 86 (2004) 1554–1563.
- [45] D. Matulis, I. Rouzina, V.A. Bloomfield, Thermodynamics of cationic lipid binding to DNA and DNA condensation: roles of electrostatics and hydrophobicity, *Journal of the American Chemical Society* 124 (2002) 7331–7342.
- [46] R. Bruinsma, J. Mashl, Long-range electrostatic interaction in DNA-cationic lipid complexes, *Europhysics Letters* 41 (1998) 165–170.
- [47] K. Wagner, D. Harries, S. May, V. Kahl, J.O. Rädler, A. Ben Shaul, Direct evidence for counterion release upon cationic lipid-DNA condensation, *Langmuir* 16 (2000) 303–306.
- [48] D.C. Rau, V.A. Parsegian, Direct measurement of temperature dependent solvation forces between DNA double helices, *Biophysical Journal* 61 (1992) 260–271.
- [49] P. Luciani, C. Bombelli, M. Colone, L. Giansanti, S.J. Ryhanen, V.M.J. Saily, G. Mancini, P.K.J. Kinnunen, Influence of the spacer of cationic gemini amphiphiles on the hydration of lipoplexes, *Biomacromolecules* 8 (2007) 1999–2003.
- [50] H. Gershon, R. Ghirlando, S.B. Guttman, A. Minsky, Mode of formation and structural features of DNA cationic liposome complexes used for transfection, *Biochemistry-USA* 32 (1993) 7143–7151.
- [51] D. Uhríková, M. Hanulová, S.S. Funari, I. Lacko, F. Devínský, P. Balgavý, The structure of DNA-DLPC-cationic gemini surfactant aggregates: a small angle synchrotron X-ray diffraction study, *Biophysical Chemistry* 111 (2004) 197–204.
- [52] C. Wang, S.D. Wettig, M. Foldvari, R.E. Verrall, Synthesis, characterization, and use of asymmetric pyrenyl-gemini surfactants as emissive components in DNA-lipoplex systems, *Langmuir* 23 (2007) 8995–9001.

- [53] M. Subramanian, J.M. Holopainen, T. Paukku, O. Eriksson, I. Huhtaniemi, P.K.J. Kinnunen, Characterisation of three novel cationic lipids as liposomal complexes with DNA, *Biochimica et Biophysica Acta Biomembranes* 1466 (2000) 289–305.
- [54] D. Hirsch-Lerner, Y. Barenholz, Probing DNA-cationic lipid interactions with the fluorophore trimethylammonium diphenyl-hexatriene (TMADPH), *Biochimica et Biophysica Acta Biomembranes* 1370 (1998) 17–30.
- [55] J. McManus, J.O. Rädler, K.A. Dawson, Phase behaviour of DPPC in a DNA-calcium-zwitterionic lipid complex studied by small angle X-ray scattering, *Langmuir* 19 (2003) 9630–9637.
- [56] O. Francescangeli, V. Stanic, L. Gobbi, P. Bruni, M. Iacussi, G. Tosi, S. Bernstorff, Structure of self-assembled liposome-DNA-metal complexes, *Physical Review E* 67 (2003) art-011904.
- [57] D. Uhríkova, M. Hanulová, S.S. Funari, R.S. Khusainová, F. Šeršeň, P. Balgavý, The structure of DNA-DOPC aggregates formed in presence of calcium and magnesium ions: a small-angle synchrotron X-ray diffraction study, *Biochimica et Biophysica Acta Biomembranes* 1713 (2005) 15–28.
- [58] E. Raspaud, C. da, F. Livolant, Do free DNA counterions control the osmotic pressure? *Physical Review Letters* 84 (2000) 2533.
- [59] Y. Wang, P.L. Dubin, H. Zhang, Interaction of DNA with cationic micelles: effects of micelle surface charge density, micelle shape, and ionic strength on complexation and DNA collapse, *Langmuir* 17 (2001) 1670–1673.
- [60] S.J. Eastman, C. Siegel, J. Tousignant, A.E. Smith, S.H. Cheng, R.K. Scheule, Biophysical characterization of cationic lipid:DNA complexes, *Biochimica et Biophysica Acta Biomembranes* 1325 (1997) 41–62.
- [61] L. Karlsson, M.C.P. van Eijk, O. Soderman, Compaction of DNA by gemini surfactants: effects of surfactant architecture, *Journal of Colloid and Interface Science* 252 (2002) 290–296.
- [62] P. Mitrakos, P.M. Macdonald, Cationic amphiphile interactions with polyadenylic acid as probed via <sup>2</sup>H-NMR, *Biochimica et Biophysica Acta Biomembranes* 1374 (1998) 21–33.